

Structural and thermal properties of PVDF/PVA blends

G. Krishna Bama · P. Indra Devi · K. Ramachandran

Received: 14 September 2008 / Accepted: 13 January 2009 / Published online: 7 February 2009
© Springer Science+Business Media, LLC 2009

Abstract Thermal properties such as thermal diffusivity and thermal conductivity are measured by photoacoustics at room temperature for various particle sizes, thicknesses and the percentage of mixing of poly (vinyl alcohol) (PVA) in Poly (vinylidene fluoride) (PVDF)/PVA blends. The results are compared with other experimental reports, which is by laser flash technique for various temperatures. The agreement is very good at room temperature; in our study, it is $0.20 \text{ Wm}^{-1} \text{ K}^{-1}$, whereas by laser flash technique it is $0.18 \text{ Wm}^{-1} \text{ K}^{-1}$ for thermal conductivity. The importance of dislocation density and strain is discussed.

Introduction

Poly (vinylidene fluoride) (PVDF), a semi-crystalline polymer is a linear fluorinated hydrocarbon with a repeat unit ($\text{CH}_2\text{-CF}_2$) with spacing of 2.6 \AA , exhibiting different crystalline phases. The β form is the one that provides the best ferroelectric properties whereas the α form is more stable [1]. PVDF and its copolymers are used for high energy density capacitors, piezo- and pyroelectric sensors because of high dielectric constant, excellent piezoelectric and pyroelectric properties. A number of detailed experimental investigations of the piezoelectric and pyroelectric and dielectric constants of PVDF have been reported in

literature [2–5]. Apart from this, polymer electrolyte studies are also carried out in PVDF [6]. However, few reports on thermal diffusion in PVDF are available in literature. Bonno et al. [7] reported the value of thermal diffusivity and thermal conductivity of PVDF film of particular thickness ($75 \mu\text{m}$) using photoacoustic (PA) technique over the temperature range $100\text{--}300 \text{ K}$ and reported that, the thermal conductivity of PVDF decreases as the temperature increases in this low temperature region.

Polymer blends have emerged as the most important areas of research as they improve chemical, physical and mechanical properties. Lim et al. [8] reported the measurement of thermal diffusivity of PVDF/PMMA (Polymethyl methacrylate) blends using heat pulse method and observed that for the PVDF content below 60 wt%, thermal diffusivity of the melt-quenched sample monotonically decreases with increasing PVDF content, which was explained by the decrease of PMMA component having higher thermal diffusivity. In this study, the isomorphous blends of two polymers PVDF and poly (vinyl alcohol) (PVA) for different wt% were prepared using solution cast technique and the effect of thickness and the particle size on the thermal properties of these mixed blends are deduced from PA measurements at room temperature.

Experimental

Sample preparation

The solution cast technique was utilized for preparing the blends PVDF and PVA. Definite compositional ratios of PVDF: PVA (90:10, 80:20, 70:30, 60:40, 50:50) were dissolved in dimethyl formamide to prepare solution. The

G. Krishna Bama (✉)
Sri Meenakshi Government College for Women,
Madurai 625 002, India
e-mail: bamavihas@rediffmail.com

P. Indra Devi · K. Ramachandran
School of Physics, Madurai Kamaraj University,
Madurai 625 021, India

solution was then heated at constant temperature of 60 °C with constant stirring. A known quantity of this solution was poured in a clean glass petri-dish and the solvent was allowed to evaporate at room temperature at least for 24 h. Similarly, pure PVDF and PVA films are prepared separately for various thicknesses using dimethylformamide and water as the solvent.

Photoacoustics

The PA technique is a non-contact method and has been used successfully to measure thermal conductivity of materials [9, 10]. The principle of this PA technique is that when a modulated light is absorbed by the sample located in a sealed PA cell, non-radiative decay of the absorbed light produces a modulated transfer of heat to the surface of the sample which produces pressure waves in the gas inside the cell, which can be detected by a microphone attached to the cell [11]. The PA spectrometer used in this work has a 400 W Xe-lamp (Jobin Yvon) mechanically chopped by an electro-mechanical chopper (Model number PAR 650) and focussed onto the sample through a monochromator (Model Triax 180, Jobin Yvon). The sample is placed in the PA cell, a non-resonant cell made up of stainless steel, and the microphone is placed very near to the sample and the PA cell. The PA signal from the microphone is fed to a lock-in amplifier (Model Perkin–Elmer 7225 DSP), and the complete set up is shown in Fig. 1.

The prepared films were then characterized by X-ray diffraction (XRD) and PA techniques at room temperature.

Results and discussion

XRD analysis

XRD patterns of PVA, PVDF and their blends PVDF/PVA are shown in Fig. 2a and b. The XRD pattern of PVA, in Fig. 2a shows a sharp peak at 19.40° indicating semi-

crystalline nature of PVA [12] whereas PVDF (Fig. 2a) shows a sharp peak at 20.01° indicating both crystalline and amorphous nature of PVDF. These results are in agreement with previously reported values in literature [12, 13]. The addition of PVA of various weight percent induces a significant disorder in the polymer structure, and hence the crystallinity of polymers. XRD pattern for all the blends PVDF/PVA shows a significant degree of crystallinity. In poly blend PVDF/PVA film, we observed a small peak in addition to that of sharp peak around $2\theta = 20^\circ$ for the ratio 50:50, which indicates that this polymer is highly crystalline compared to all the other blends. In poly blend of 60:40, we observed a broad peak at 19.98° which indicates that this polymer is more amorphous compared to all the other blends. From XRD data, the average particle size, dislocation density and strain for PVA, PVDF and PVDF/PVA blends were estimated using Eqs. 1, 2 and 3 and the corresponding values are given in Tables 1 and 2. Bhajantri et al. [12] studied the effect of BaCl₂ dopant on the optical and microstructural properties of PVA and reported the average crystallite size using the observed wide angle X-ray diffraction (WAXD) data (of thickness 0.05–0.2 mm) and Scherrer’s equation as 2.92 nm. In our study, we have calculated the particle size for pure PVA films (of thickness 23–95 μm) with Scherrer’s equation as 7–24 nm.

Assuming that all the grains are of arbitrary shape, their sizes may be determined from Debye Scherrer formula. For pseudo-Voigt function calculation particles will be complicated and Debye Scherrer [14] have obtained the particle size as

$$d = K_{hkl}\lambda/\beta \cos \theta \tag{1}$$

where K_{hkl} is the Scherrer’s constant depending on the shape of the particle, β is the integral width of the Bragg reflection, exactly equal to full width at half maximum (FWHM) when the reflections are in the form of rectangle and triangle, λ is the wavelength of X-ray and θ is the diffraction angle.

The dislocation density (ρ) of the films was calculated using the relation

$$\rho = 1/d^2 \tag{2}$$

where d is the particle size of the film.

The strain parameter (η) was calculated from the equation

$$\eta = [\lambda/d \cos \theta - \beta \times \pi/180]1/\tan \theta \tag{3}$$

From Table 1, it is seen that as thickness of the film increases, dislocation density and strain are found to increase. For higher thickness, the particle size will be bigger, so the strain (from bulk) is small which is seen here. If diffraction angles are very small, then $K_{hkl} = 0.9$ when the powder is homogeneous. Large particle size, absence of

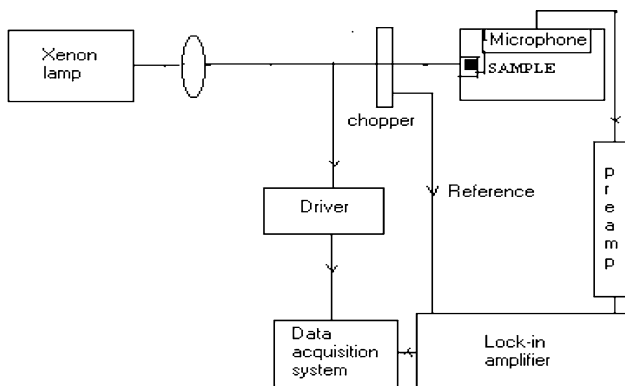


Fig. 1 Schematic diagram of photoacoustic spectrometer

Fig. 2 **a** XRD spectra of: (1) PVA, (2) PVDF, **b** XRD spectra of PVDF: PVA : (1) 90:10, (2) 80:20, (3) 70:30 (4) 60:40, (5) 50:50,

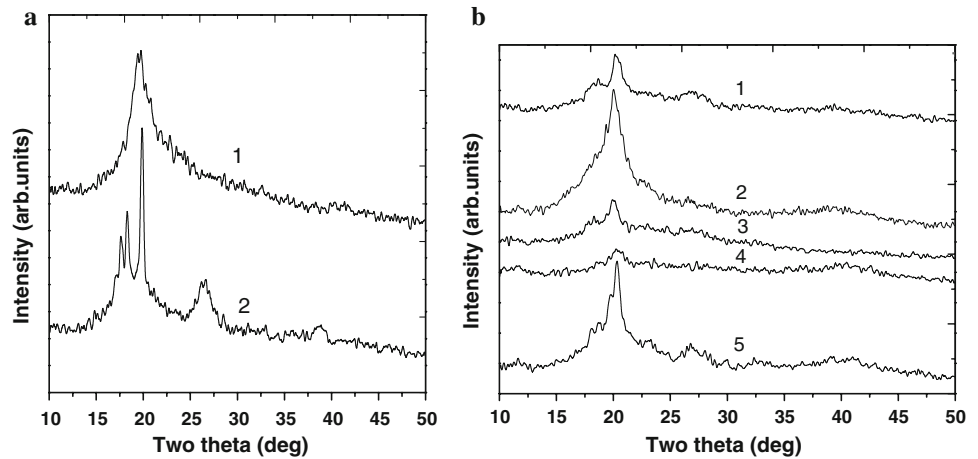


Table 1 Calculated value of particle size, dislocation density and strain for pure PVA and PVDF films (error $\sim \pm 1\%$)

Sample	Thickness (μm)	Particle size (nm)	Dislocation density ($\rho \times 10^{15}$ lines/ m^2)	Strain ($\eta \times 10^{-3}$)
PVA	95	24	1.67	1.72
	47	10	8.73	5.30
	23	7	19.67	7.75
PVDF	200	34	0.86	1.66
	120	28	1.23	1.87
	70	29	1.23	1.88

Table 2 Calculated value of particle size, dislocation density and strain for and PVDF/PVA blends (error $\sim \pm 1\%$)

PVDF/PVA	Thickness (μm)	Particle size (nm)	Dislocation density ($\times 10^{15}$ lines/ m^2)	Strain ($\times 10^{-3}$)
90:10	254	17	3.41	1.56
80:20	150	23	1.82	2.27
70:30	50	14	4.91	3.73
60:40	197	8	13.61	6.09
50:50	231	19	2.76	2.76

strain distortions and the homogeneity of the composition of these specimens would lead to the broadening of the reflections. When broadening is very small, strain due to in homogeneity and small particle (grain) size should always be considered as it determines the stability (mechanical and thermal) of the sample. Similarly, deformation distortions and induced non-uniform displacement of the atoms from lattice sites would lead to random distortion of dislocations in the volume of the specimen, as the displacements of the atoms are determined by the super position of displacement from every dislocation. These will also contribute to the broadening of the diffraction. Therefore, dislocation density and strain are monitored when the size of particles (grains) become smaller and smaller. In Table 2

we could see a maximum in the strain and dislocation density when the particle size is 8 nm, even though thickness is 197 μm . Therefore, if we want very small size of the particle (say, below 8 nm), it is better to have smaller thickness for mechanical stability. Only for these reasons, dislocation density and strain values are given in Table 2.

Thermal diffusivity

For measuring thermal diffusivity, pure PVDF, PVA and poly blends PVDF/PVA are taken separately inside the PA cell, and the PA signal is observed for different chopping frequencies keeping the wavelength fixed. Thermal diffusivity was determined from the thermal diffusion model of the PA effect which states that for an optically opaque and thermally thick sample the pressure fluctuations are given by,

$$dp = \gamma p_0 I_0 (\alpha_g \alpha_s)^{1/2} \exp j(\omega t - \pi/2) / 2\pi T_0 l_g K_s f \sinh(l_s \sigma_s) \quad (4)$$

where γ is the specific heat ratio of air, p_0 the ambient pressure, I_0 the incident light beam intensity, T_0 the room temperature, f the chopping frequency and l_i , K_i , and α_i are the thickness, thermal conductivity, and thermal diffusivity of material i , respectively. The subscript i denotes either sample (s) or gas (g) and $\sigma_i = (1 + j)a_i$ with $a_i = (\pi f / \alpha_i)^{1/2}$ is the complex thermal diffusion coefficient of material 'i'.

Particularly, for an optically opaque and thermally thick sample ($l_s \sigma_s \gg 1$), the expression for the PA amplitude is given by [11],

$$S = \exp(-af^{1/2}) A/f \quad (5)$$

where the constant A , apart from geometric constants, include factors such as the light intensity, room temperature, gas thermal properties and

$$a = (\pi l_s^2 / \alpha_s)^{1/2} \tag{6}$$

$$K = \alpha \rho C_p \tag{7}$$

From the slope of $\ln(f \cdot S)$ (where f is the chopping frequency and S is the photoacoustic amplitude) as a function of $f^{1/2}$, we deduce the thermal diffusivity, α_s , of the sample from this relation $a = (\pi l_s^2 / \alpha_s)^{1/2}$ where l_s is the thickness of the sample. The graphs are shown in Fig. 3a–f. Thermal conductivity of the sample is then found out using the relation

where ρ is the density, C_p is the specific heat capacity and α is the thermal diffusivity of the sample.

The measured values of thermal diffusivity of pure PVA, PVDF and the blends of PVA/PVDF films are given in Tables 3 and 4. From Table 3 it may be seen that, with a decrease in thickness of PVDF and PVA films, their particle size decreases while their thermal diffusivity

Fig. 3 **a** Depth profile spectrum of pure PVA of thickness 95 μm , **b** Depth profile spectrum of the blend PVDF/PVA (90:10), **c** Depth profile spectrum of the blend PVDF/PVA (80:20), **d** Depth profile spectrum of the blend PVDF/PVA (70:30), **e** Depth profile spectrum of the blend PVDF/PVA (60:40), **f** Depth profile spectrum of the blend PVDF/PVA (50:50)

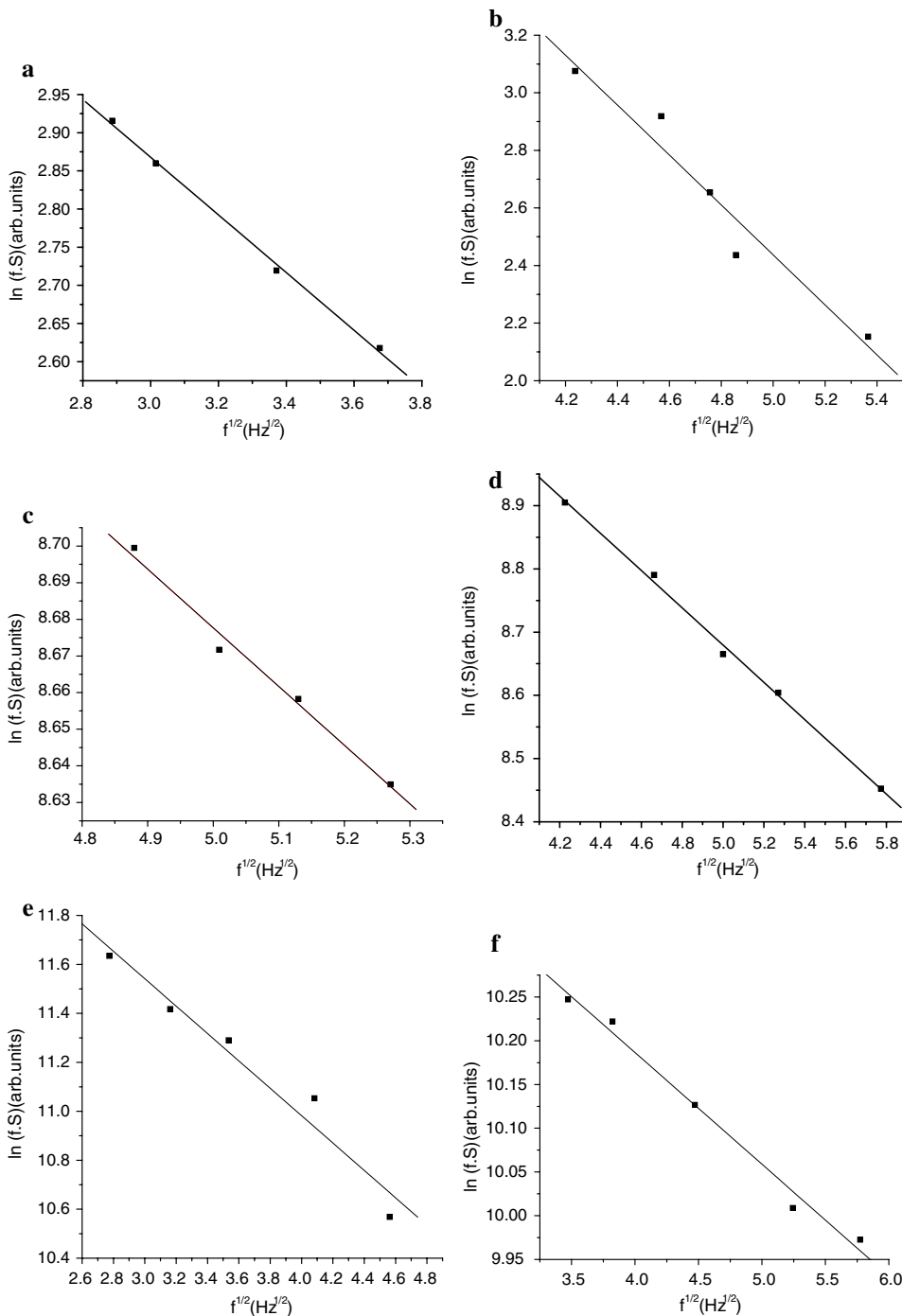


Table 3 Thermal properties of pure PVA and PVDF films (error $\sim \pm 1\%$)

Sample	Thickness (μm)	Particle size (nm)	Thermal diffusivity ($\times 10^{-7} \text{ m}^2 \text{ s}^{-1}$)	Thermal conductivity ($\text{Wm}^{-1} \text{ K}^{-1}$)
PVA	95	24	1.9	0.34
	47	10	2.2	0.39
	23	7	2.6	0.46
PVDF	200	34	0.58	0.15
	120	29	0.79	0.20
	70	28	0.93	0.23

Table 4 Thermal properties of PVDF/PVA film (error $\sim \pm 1\%$)

PVDF/PVA	Thickness (μm)	Particle size (nm)	Thermal diffusivity (PA technique) ($\times 10^{-7} \text{ m}^2 \text{ s}^{-1}$)	Thermal conductivity (PA technique) ($\text{Wm}^{-1} \text{ K}^{-1}$)
90:10	254	17	0.79 (0.74)	0.21 (0.24)
80:20	150	23	0.95 (0.88)	0.21 (0.30)
70:30	50	14	1.00 (1.03)	0.22 (0.36)
60:40	197	8	1.35 (1.16)	0.31 (0.42)
50:50	231	19	1.67 (1.13)	0.37 (0.49)

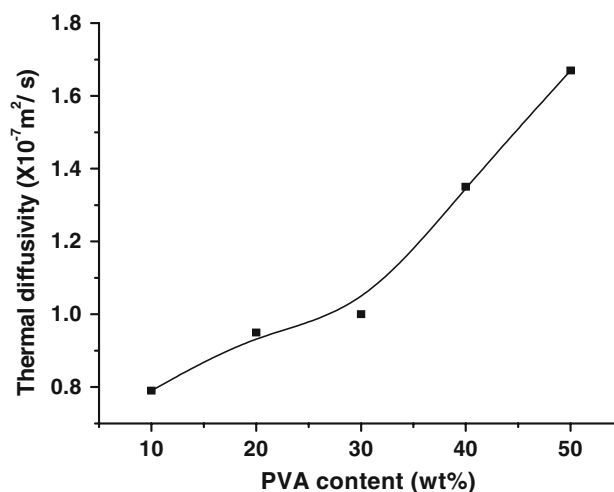
increases. This can be understood as follows: as the particle size of the sample increases there will be a decrease in mean free path due to increase in phonon collision rate which reduces thermal diffusivity. However, a direct comparison cannot be made for PVDF and PVA films, because the number of monomers for the thickness of the investigated film is not known. Bonno et al. [7] reported the value of thermal diffusivity and thermal conductivity of PVDF film of particular thickness ($75 \mu\text{m}$) using PA technique as $6 \times 10^{-8} \text{ m}^2 \text{ s}^{-1}$ and $0.16 \text{ Wm}^{-1} \text{ K}^{-1}$. Our results are in agreement with the value reported by Bonno et al. [7] within the error limit.

Santos et al. [15] have recently reported measurements on thermal properties of PVDF in the temperature range of 298–483 K by laser flash technique. Even though the melting point of PVDF is 446 K, they have made the measurements even beyond the melting point, whereas we compared our results only with the results at room temperature. For example, from literature [7, 15, 16], thermal diffusivity was found to be in the range of $0.03\text{--}0.09 \times 10^{-6} \text{ m}^2 \text{ s}^{-1}$ and thermal conductivity the range of $0.14\text{--}0.18 \text{ Wm}^{-1} \text{ K}^{-1}$, whereas Santos et al. [15] have observed them as $0.1115 \times 10^{-6} \text{ m}^2 \text{ s}^{-1}$ and $0.2620 \text{ Wm}^{-1} \text{ K}^{-1}$, respectively at room temperature. Our values are $0.093 \times 10^{-6} \text{ m}^2 \text{ s}^{-1}$ and $0.23 \text{ Wm}^{-1} \text{ K}^{-1}$ for an averaged particle size of 28 nm and thickness of the film is 0.07 mm at room temperature. Santos et al. [15] have used a film of thickness about 0.5 mm. Thickness alone cannot determine the thermal diffusivity as

the particle size also plays an important role as seen in our earlier studies [17]. When thickness is reduced, the chance of multiple scattering by nanoparticles will be inevitable which would lead to a reduction in mean free path and hence the thermal conductivity. This is the reason for the small deviation of our value with Santos et al. [15]. In the absence of data for strain and dislocation density of PVDF from the study of Santos et al. [15], we cannot do a one-to-one comparison for thermal conductivity. But within the error limit, we see a good agreement with the observed values of thermal properties between laser flash technique [15] and PA technique (this study).

Fumiaki et al. [18] performed in- and cross-plane thermal diffusivity measurements of commercially available polyimide films for various thicknesses using the ac-calorimetric distance-variation method and the temperature wave analysis method. In both the advanced and standard polyimide films, in-plane thermal diffusivity decreases slightly but clearly as the film becomes thicker. The same trend is observed in this study results.

The results on thermal diffusivity (α) of the polymer blend shows (Table 4) that as the content of PVA is increased, thermal diffusivity is found to increase and it reaches a maximum when the blends are in equal proportion. Since heat transfer in the crystalline region is faster than that in the non-crystalline (amorphous) region, the crystallization causes the increase of α . XRD analysis also shows that this poly blend (50:50) is highly crystalline compared to all the other blends. It is also seen that, α of the poly blend (PVDF/PVA) increases with increasing PVA content as shown in Fig. 4. To the best of our knowledge, the thermal diffusivity and thermal conductivity values of the poly blends PVDF/PVA are not available in literature, and hence, a direct comparison could

**Fig. 4** Dependence of thermal diffusivity of PVA/PVDF blends on their molar composition

not be made. However, the results are compared with the calculated values using Vegard's law as follows;

$$\alpha_{\text{PVDF/PVA}} = \chi\alpha_{\text{PVA}} + (1 - \chi)\alpha_{\text{PVDF}} \quad (8)$$

where α_{PVA} and α_{PVDF} are the known values of thermal diffusivity of pure PVA and PVDF film, respectively (taken from literature [7, 19]), $\alpha_{\text{PVDF/PVA}}$ is the calculated thermal diffusivity of the polymer blend PVDF/PVA using this relation, and χ is the mole fraction of the polymer used.

It is found that the results are in agreement with that of calculated values as shown in Table 4. It has been reported that the effective thermal diffusivity of composites depend on the thermal diffusivity of constituents as well as on their relative volume fraction [20]. In this case also, the composites of PVDF and PVA exhibit a thermal diffusivity the value which is intermediate (thermal diffusivity of the films PVDF and PVA are $0.60 \times 10^{-7} \text{ m}^2 \text{ s}^{-1}$ and $2.2 \times 10^{-7} \text{ m}^2 \text{ s}^{-1}$, respectively) to that of pure PVDF and PVA.

Conclusion

Thermal diffusivity and thermal conductivity of the poly blends are studied for various particle sizes, and hence thicknesses. The size of the particles vary from 8 nm to 23 nm, which are quite different from Bhajantri et al. [9], where a particle size 2.92 nm is reported for poly vinyl alcohol. It is not reasonable to use Debye Scherrer formula to find the size of the particles when they are around 1 nm, and so in this study, we concentrate only on our results and not on Bhajantri et al. [9]. As the percentage of PVA increases in PVDF thermal diffusivity increases systematically as in Table 4, which is also found to obey Vegard's law. But there is no systematic variation in particle size and thickness as the PVA content increases. This is because no capping agent is added in the polymer blends so, only

composition will determine the thermal properties. Essentially, only the PVA concentration determines the thermal properties in this study in the PVDF/PVA blends.

Acknowledgements One of the authors (G. Krishna Bama) acknowledges University Grants Commission, New Delhi for providing a fellowship under FIP scheme to carry out this study in the School of Physics, Madurai Kamaraj University, Madurai.

References

1. Yamadat T, Mizutani T, Ieda M (1982) *J Phys Appl Phys* 15:289
2. Fukada E, Furukawa T (1981) *Ultrasonics* 19:31
3. Sessler GM (1981) *J Acoust Soc Am* 70:1596
4. Singh R, Kumar J, Rajiv K et al (2006) *Polymer* 47:5919
5. Kubouchi Y, Kumetani Y, Yagi T et al (1989) *Pure Appl Chem* 61:83
6. Rajendran S, Sivakumar P, Shanker babu R (2006) *Bull Mater Sci* 29:673
7. Bonno B, Laporte JL, Tascón d'León R (2001) *Meas Sci Technol* 12:671
8. Lim J, Kim J, Yu K et al (1998) *J Korean Phys Soc* 32:S228
9. Zammit U, Marinelli M, Pizzoferrato R et al (1988) *J Phys E Sci Instrum* 21:935
10. Delgado-Vasallo O, Marin E (1999) *J Phys D Appl Phys* 32:593
11. Rosencwaig A (1980) *Photoacoustics and photoacoustic spectroscopy*. Wiley, New York
12. Bhajantri RF, Ravindrachary V, Harish et al (2006) *Polymer* 47:3591
13. Gupta AK, Bajpai R, Keller JM (2006) *J Mater Sci* 41:5857. doi: [10.1007/s10853-006-0359-2](https://doi.org/10.1007/s10853-006-0359-2)
14. Zidan HM (2003) *J Appl Polym Sci* 88:1115
15. Dos Santos WN, Iguchi CY, Gregorio R (2008) *Polym Test* 27:204
16. Balderas-Lopez JA, Fonseca MRJ, San Martin E et al (2005) *J Phys IV* 25:669
17. Raji P, Sanjeeviraja C, Ramachandran K (2005) *Bull Mater Sci* 28(3):233
18. Takahashi F, Katsuyoshi I, Morikawa J et al (2004) *Jpn J Appl Phys* 43:7200
19. Giglio M, Vendramini A (1977) *Phys Rev Lett* 38:26
20. George D, Saravanan S, Anantharaman MR et al (2004) *Phys Rev B* 69:235201